Journal of Materials and Environmental Sciences
ISSN : 2028-2508
CODEN : JMESCN

J. Mater. Environ. Sci., 2018, Volume 9, Issue 3, Page 1051-1057

https://doi.org/10.26872/jmes.2018.9.3,117

http://www.jmaterenvironsci.com

Synthesis, Characterization and Application of Chromium Molybdate for Oxidation of Methylene Blue Dye

Hicham Oudghiri-Hassani [1,2*]

[1] *Taibah University, College of Science, Chemistry Department, Almadinah 30002 Saudia Arabia.*
[2] *Cégep de Drummondville, Département Sciences de la nature, 960 rue Saint-Georges, Drummondville, Québec, Canada J2C 6A2.*

Received 04 Dec 2017,
Revised, 17 Dec 2017
Accepted 19 Dec 2017

Keywords
- ✓ *Chromium molybdate,*
- ✓ *Nanoparticles,*
- ✓ *Catalysis,*
- ✓ *Dye oxidation.*

oudghiri_hassani_hicham@yahoo.com
Phone: +966543549454

Abstract

Chromium molybdate $Cr_2(MoO_4)_3$ nanoparticles were synthetized via heating an oxalate precursor in static air at 600 °C. The precursor was studied by thermal gravimetric analysis (TGA), and it was analyzed by Fourier transform-Infrared radiation (FT-IR) spectrometer. The synthesized chromium molybdate was analyzed by Brunauer–Emmett–Teller technique (BET), transmission electron microscopy (TEM), and X-ray diffraction (XRD), and its catalytic activity was tested. Chromium molybdate exhibits an efficiency in the catalytic oxidation and degradation of methylene blue with hydrogen peroxide. The oxidation was controlled using UV visible absorption measurements.

1. Introduction

Dyes are essential compounds used in various industries such as paper, leather, textile and plastic manufacture [1]. However, it pollutes the environment by the generation of coloured wastewater.

Therefore, several methods (photocatalysis, biological, physical, and chemical) were applied to remove and degrade the hazardous organic dyes from contaminated wastewater [2-8]. Among all techniques, chemical method using oxidation reaction under or without UV light in the presence of catalyst was a simple and rapid process that can degrade the toxic dye compounds [9].

In past decades, metal molybdate compounds with the formula $MMoO_4$ or $M_2(MoO_4)_3$ are one of the most important families of inorganic materials that have interesting applications in various fields. Most of the applications are industrial catalysts for partial oxidation of hydrocarbons or catalysts in the hydrodesulfurization (HDS) process, scintillator materials, humidity sensors, photoluminescence, optical fibers, scintillator materials, humidity sensors and photo-catalysis [10-11], microwave application, electrochemical and magnetic properties. Nowadays, different compounds of molybdates such as iron molybdate [12], zinc molybdate [13, 14], cobalt molybdate [15], nickel molybdate [16–19], europium molybdate [20], cadmium molybdate [21], etc. have been synthesized in nanoscale.

In particular, nanostructured chromium molybdate, has special magnetic, electrical and catalytic properties [22, 23], and is the most promising catalysts for selective oxidation of methanol [24].

Chromium molybdate is prepared by several methods: precipitation method [22], solid-state synthesis [25], or thermal decomposition of chromate and molybdate sols [26-27]. The synthesis methods of the compound influence its properties significantly.

In this study, nanostructured $Cr_2(MoO_4)_3$ catalyst was prepared via the thermal decomposition of an oxalate precursor prepared in the solid state using a new method. The obtained powder was composed of nanoparticles. The freshly synthesized $Cr_2(MoO_4)_3$ nanoparticles were tested as catalysts for the oxidation and degradation of methylene blue dye with hydrogen peroxide.

2. Material and Methods

2.1. Synthesis of chromium molybdate

Chromium molybdate catalyst was synthesized as follows. Initially, the solid state reaction on a hotplate at 160 °C of a ground mixture of oxalic acid $H_2C_2O_4,2H_2O$, ammonium molybdate $(NH_4)_6Mo_7O_{24},4H_2O$, and

chromium nitrate $Cr(NO_3)_3,9H_2O$ in the molar ratio 10 /0.43 /2 [28] leads to the formation of an oxalate precursor.

The change of color for the chromium molybdenum precursor from white to dark gray, and the formation of NO_2 through an orange/brownish gas evolved during heating are evidence of the reduction reactions produced in the mixture. In fact, the acid plays simultaneously important roles as a complexing ligand of chromium and molybdenum and as reducing agent of nitrate anions and of molybdenum according to the mechanism presented by the following equations 1 and 2.

$$NO_3^- + 4\,H^+ + 3e^- \longrightarrow NO + 2H_2O \quad (1)$$

$$NO + \tfrac{1}{2}\,O_2 \longrightarrow NO_2 \quad (2)$$

Finally, a thermal decomposition of the mixture under static air at 600 °C for two hours was realized to obtain the final oxide [29-30].

2.2. Characterization

A thermal gravimetric analysis using a SDT Q 600 instrument analyzed the precursor in the first step. While the X-ray diffraction were used to record the patterns in the range of 10° to 80° in 2θ in the second step using a Shimadzu X-ray diffractometer 6000 equipped with a Ni filter and a Cu-Kα radiation (1.5406 Å) source. In proposing that the particles are spherical we calculated the particle size with the equation $D_{XRD} = 0.9\ \lambda/ (B \cos\theta)$, where λ is the Cu-Kα wavelength, θ is the Bragg angle, and B is the full width at half maximum (FWHM) expressed in radians. A Micromeritics ASAP 2020 surface area and porosity analyzer was used to obtain the adsorption desorption isotherms. A Shimadzu 8400S apparatus was used to study an infrared spectroscopy. Transmission electron microscopy (TEM) using a JEM – 1400 Flash electron microscope operated at 120 kV was used to investigate the shape and size of the particles, while a UV visible absorption spectrophotometer (Varian Cary 100) was performed to measure the variation of the methylene blue concentrations during the oxidation and degradation with hydrogen peroxide.

2.3. Test of methylene blue oxidation

The catalytic achievement of chromium molybdate was tested in the oxidation and degradation of methylene blue. In fact, both 45 ml of methylene blue 5ppm, and 5 ml of hydrogen peroxide 33 wt. % was mixed into an aqueous solution under continuous stirring at 23 °C. The mixture was a dark blue color with an absorption peak located at 665 nm. The chromium molybdate (0.1 g) was added to the solution under stirring. The action of the catalyst was observed by changing the color of the solution with a gradual decrease from dark blue to light blue, leading to the total discoloration after 24 hours. The reaction was followed by ultraviolet-visible (UV-Vis) spectrophotometer.

3. Results and discussion

3.1. Characterizations of the precursor

The results of the reaction between ammonium molybdate $(NH_4)_6Mo_7O_{24},4H_2O$, chromium nitrate $Cr(NO_3)_3,9H_2O$, and oxalic acid at 160°C was analyzed by the Fourier transform infrared spectroscopy (FTIR) and presented in Figure 1.

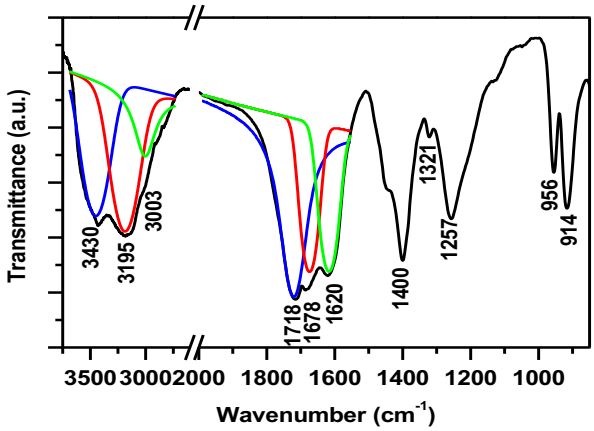

Figure 1: FTIR spectrum of mixture after heated at 160 °C.

According to the results found in the literature, the spectrum shows the bands of the coordinated oxalate group [31]. The presence of bands at 1718 cm^{-1} and 1678 cm^{-1}, can be assigned to the C=O vibration of the oxalate group. The band at 1400 cm^{-1} provides another proof of the presence of the C–O stretch. While, the band located at 1321 cm^{-1} can be assigned to υ(C–O) and δ (OCO) [32].
The band attribute to the hydroxyl of water occurs around 3430 cm^{-1}, and the band at 1620 cm^{-1} corresponding to δ(H_2O) indicating that the H_2O is not coordinated to the metal [33]. Besides the absorption bands due to the coordinated oxalate group, and the water, the compound shows fairly strong bands at 914 cm^{-1} and 956 cm^{-1} which can be assigned to the Mo=O stretch [32]. The spectrum reveals also the presence of strong bands at 3195 cm^{-1} and 3003 cm^{-1} due to the stretched vibration of NH_4^+ ion [34]. Over more, a band is observed at 1257 cm^{-1}, which is a good evidence of the presence of NH_4^+ion [34].
The thermogravimetric analysis of chromium molybdate was experimented to determine the amount of weight loss in the obtained precursor when heated in dry air and the results are shown in Figure 2. The thermal gravimetric curve can be divided in three steps; the first mass lost weight is between 25 °C and 150°C corresponding to 33% due to water existing in the initial precursor. The IR spectroscopy studies described above confirmed the presence of water. The second step until 320°C, show a rapid loss centered at 250 °C, corresponding to the decomposition of the precursor. While, the last step between 320°C and 425°C described a small loss. So, the total weight loss is 73%. No weight loss was observed beyond 450 °C. The temperature of 600 °C was chosen to obtain the chromium molybdate oxide by the calcination of the precursor in air.

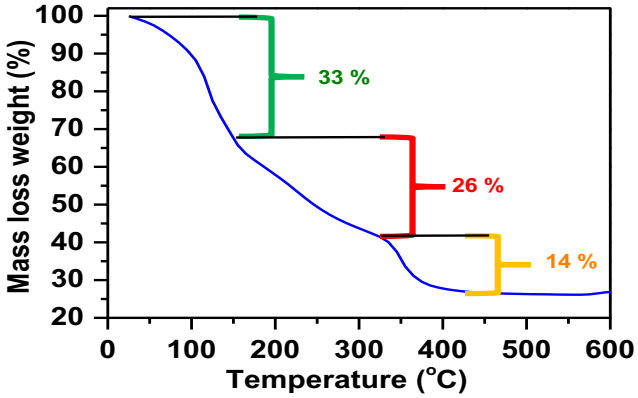

Figure 2: TGA of the chromium molybdate precursor.

3.2. Characterizations of chromium molybdate
3.2.1 X-ray diffraction
Figure 3, shows the XRD pattern of the calcined precursor sample at 600 °C which reveals the presence of $Cr_2(MoO_4)_3$.

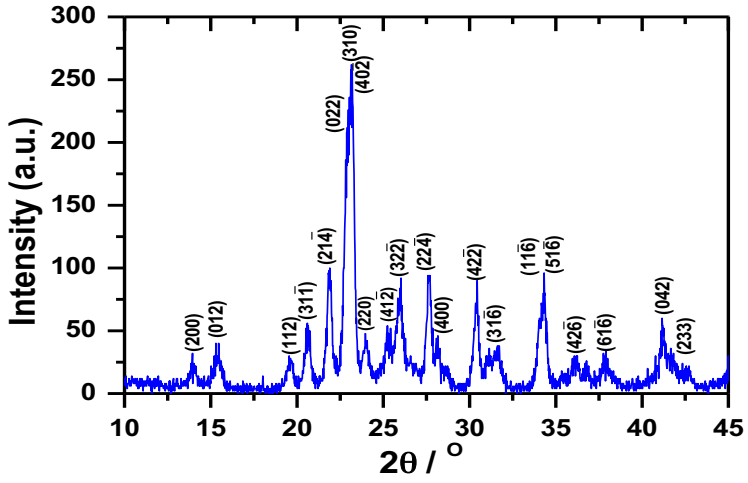

Figure 3: XRD pattern of $Cr_2(MoO_4)_3$.

The XRD pattern is indexed according to the J.C.P.D.S. file number 78-1654, corresponding to the monoclinic phase of the chromium molybdenum oxide that crystallizes with the parameters a = 15.569(4) Å, b = 9.1707(4) Å, and c = 18.141(3) Å and β = 125.390(1)° with space group $P2_1/a$. The peak located at 2θ= 21.88° was chosen to estimate the crystallite size D_{XRD}, and 43 nm was the number that was found.
Therefore, to verify if the product is pure crystalline compound or not, the FTIR was used (Fig.4). The obtain spectrum reveals the presence of the high frequency band at 970 cm^{-1} which is due to vibrations of the distorted MoO_4 tetrahedral building the $Cr_2(MoO_4)_3$ crystal structure. The bands located at 870 and 820 cm^{-1} are assigned to stretching vibrations of (Mo-O-Mo). The result is similar to that obtained in the previous studies of chromium molybdate by D. Klissurki et al. [35]. Therefore, the XRD and FTIR show that the synthesized product was a pure crystalline chromium molybdate.

3.2.2 Specific surface area measurement
To determine the specific surface area of the $Cr_2(MoO_4)_3$, the BET adsorption desorption of the liquid nitrogen was used and represented in Figure 5. Table 1 shows the specific surface area, the pore volume and the average pore size with the detailed parameters.

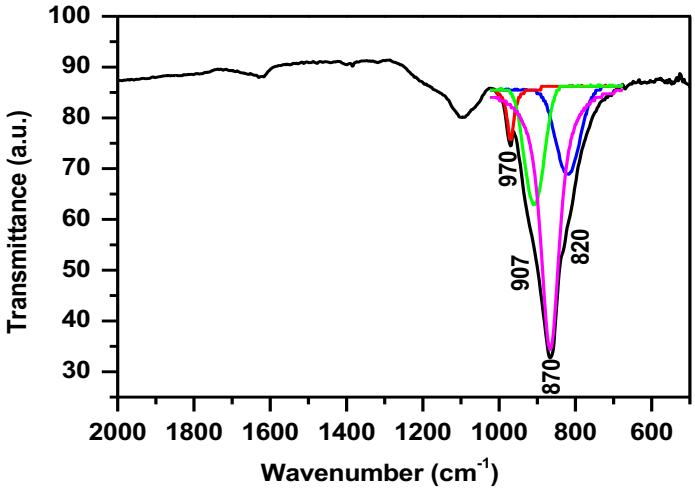

Figure 4: FTIR spectrum of $Cr_2(MoO_4)_3$ final product.

Table 1: BET result of chromium molybdate.

	S_{BET} * (m^2/g)	Pore volume ** (cm^3/g)	Average pore size** (Å)
$Cr_2(MoO_4)_3$	1.977	0.00312	63.13

(*): The BET surface area was calculated by using the adsorption in P/P_0 range from 0.1 to 0.3.
(**) : Pore volume and average pore size were found using the desorption in P/P_0 = 0.975885886.

3.2.3 Micrographs of chromium molybdate
The micrographs of $Cr_2(MoO_4)_3$ synthetized are presented in Figures 6 (a, b). Figure 6a shows agglomerated spherical particles of chromium molybdate approximately of 80 nm in diameter. The agglomerates are approximately of 2 to 3 microns (Figure 6b). The particle size of chromium molybdate obtained by TEM technique is not ascertained by the XRD analysis. In fact, XRD measures the crystallite size instead of the particle size, which explains the 43 nm value of the particle size calculated from the X-ray diffraction analysis. The formation of greater particles size is due to the agglomeration of the crystallites. XRD calculation of the crystallite size is not affected by the large particle size resulting from particles agglomeration because the crystallites are separately crystallized.

3.3 Oxidation of methylene blue
The catalytic efficiency of the chromium molybdate was investigated in the oxidation and decomposition of methylene blue dye with hydrogen peroxide under specific conditions. The variation of the concentration of methylene blue with time during the progress of the reaction was followed by measuring the methylene blue absorbance at the peak wavelength λ_{max} = 665 nm.

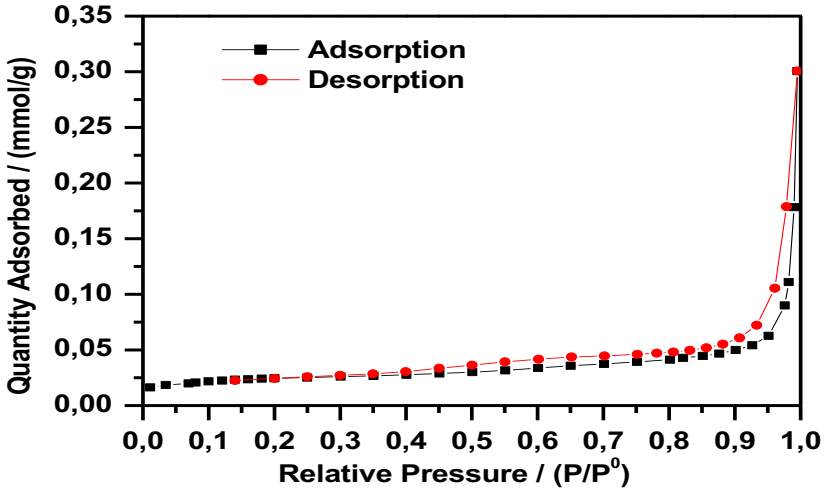

Figure 5: BET surface area plot of $Cr_2(MoO_4)_3$.

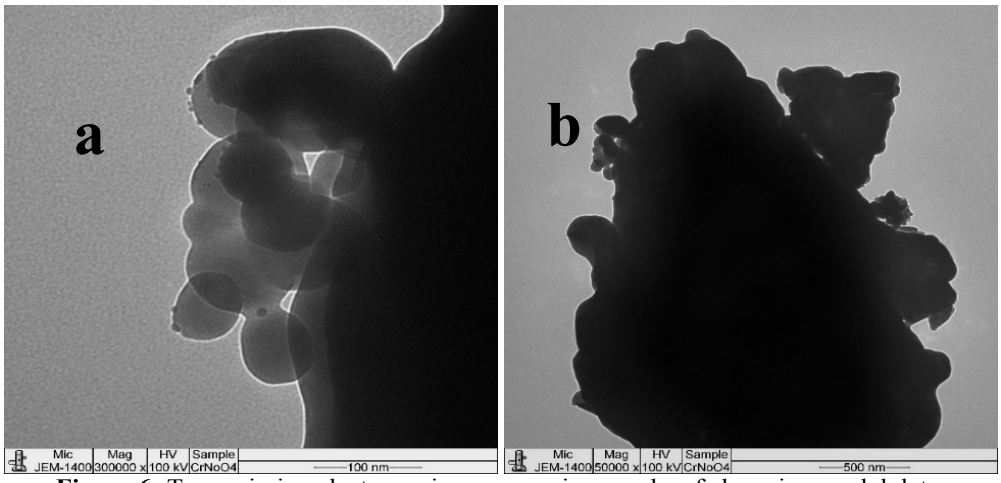

Figure 6: Transmission electron microscopy micrographs of chromium molybdate.

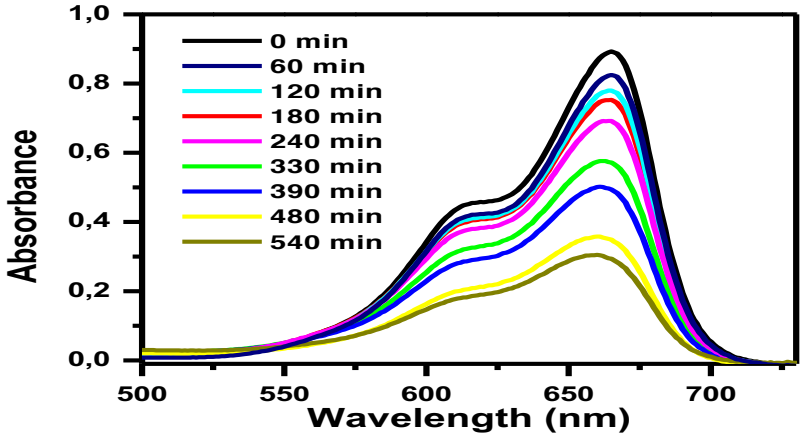

Figure 7: Time resolved spectra for the reaction of 5 ppm of methylene blue with H_2O_2 33 wt. % and 0.1 g $Cr_2(MoO_4)_3$ at 23°C.

Figure 8, represents the variation of methylene blue concentration as a function of time after adding the catalyst $Cr_2(MoO_4)_3$. This Figure shows that after 540 min of reaction, the concentration of pure methylene blue had not changed. While, the oxidation of the methylene blue by hydrogen peroxide without catalyst had a small decrease

of about 3% in the first contact and stay unchanged during the time. However, in the presence of the chromium molybdate the absorbance at 665 nm decreases with time till 30% inducing the oxidation of methylene blue. After 24 hours, the coloration of the solution becomes yellow without any change in the coloration of the chromium molybdate powder. This result demonstrates the good catalytic efficiency of the synthesized $Cr_2(MoO_4)_3$.

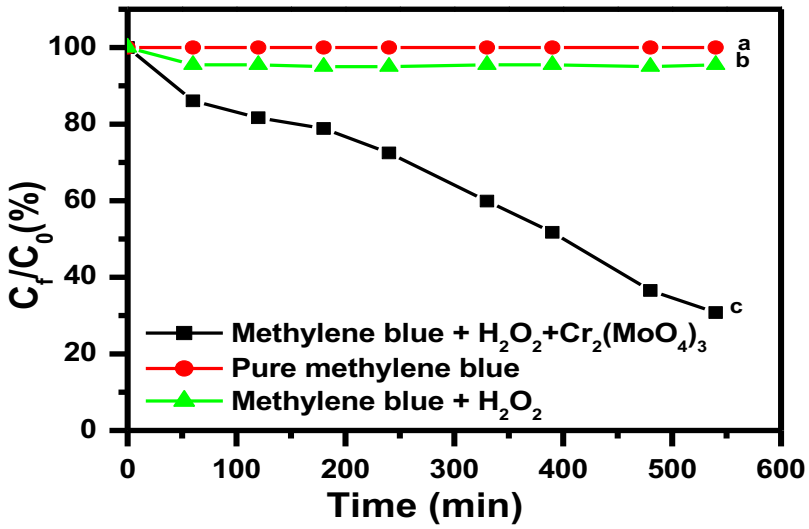

Figure 8: The change of methylene blue concentration as a function of time after adding $Cr_2(MoO_4)_3$ a) Pure methylene blue. b) Methylene blue and hydrogen peroxide. c) Methylene blue, hydrogen peroxide and $Cr_2(MoO_4)_3$.

Conclusion

The chromium molybdate nanoparticles were successfully prepared using a simple method. $Cr_2(MoO_4)_3$ were prepared at a relatively low temperature from a reacted mixture of chromium nitrate, ammonium molybdate and oxalic acid at 160 °C, that was heated in static air at 600 °C. The resulting material nanoparticles were characterized by XRD, BET, and TEM. The efficiency of the synthesized catalyst was tested in the oxidation and degradation of methylene blue. These results make the chromium molybdate as a good candidate for the oxidation of organic dyes.

References

1. S. Barreca, S. Orecchio, A. Pace, *Appl. Clay Sci*. 99 (2014) 220–228.
2. C. Tocchi, E. Federici, L. Fidati, R. Manzi, V. Vincigurerra, M. Petruccioli, *Water Res.* 46 (2012) 3334–3344.
3. A. Dbrowski, Z. Hubicki, P. Podkocielny, E. Robens, *Chemosphere.* 56 (2) (2004) 91–106.
4. A.K. Verma, R.R. Dash, P. Brunia, *J. Environ. Manage.* 93 (2012) 154–168.
5. D.J. Ennigrou, L. Gzara, M.R. Ben Romdhane, Dhahbi, *Desalination.* 246 (1-3) (2009) 363–369.
6. I. Hachoumi, I. El Ouahabi, R. Slimani, B. Cagnon, M. El Haddad, El Antri, S. Lazar, *J. Mater. Environ. Sci.* 8 (4) (2017) 1448–1459.
7. B. Mondal, V.C. Srivastava, J.P. Kushawaha, R. Bhatnagar, S. Singh, I.D. Mall, *Sep. Purif. Technol.* 109 (2013) 135–143.
8. M.H. El-Naas, S. A. Al-Muhtaseb, S. J. Makhout, *Hazard. Mater.* 164 (2009) 720–725.
9. M. Liu, Y. Wang, Z. Cheng, M. Zhang, M. Hu, J. Li, *Appl. Surf. Sci.* 313 (2014)360-367.
10. E. Karaoglu, A. Baykal, *J. Supercond Nov. Magn*. 27 (2014) 2041−2047.
11. L. Wang, H. Wang, A. Wang, M. Liu, *Chinese J. Catal.* 30 (2009) 939−944.
12. H. Oudghiri-Hassani, *Catal. Commun.* 60 (2015) 19–22.
13. G. Zhang, S. Yu, Y. Yang, W. Jiang, S. Zhang, B. Huang, *J. Cryst. Growth* 312 (2010) 1866-1874.
14. M.A. Patel, B.A. Bhanvase, S.H. Sonawane, *Ultrason. Sonochem.* 20 (2013) 906-913.
15. K. Eda, Y. Uno, N. Nagai, N. Sotani, M.S. Whittingham, *J. Solid State Chem.* 178 (2005) 2791-2797.
16. G. Kianpour, M. Salavati-Niasari, H. Emadi, *Ultrason. Sonochem.* 20 (2013) 418-424.
17. P. Liu, Y. Deng, Q. Zhang, Z. Hu, Z. Xu, Y. Liu, M. Yao, Zh Ai, *Ionics* 21 (2015) 2797-2804.

18. J. Haetge, I. Djerdj, T. Brezesinski, Nanocrystalline. *Chem. Commun.* 48 (2012) 6726-6728.
19. M. Dhanasekar, S. Ratha, C. SekharRout, S. VenkataprasadBhat, *J. Environ. Chem. Eng.* 5 (2017) 2997-3004.
20. S.M. Pourmortazavi, M. Rahimi-Nasabadi, Y. Azli, M. Mohammad-Zadeh, *Appl. Phys. A* 119 (2015) 929-936.
21. Z. Shahri, A. Sobhani, M. Salavati-Niasari, *Mater. Res. Bull*. 48 (2013) 3901-3909.
22. S. Verma, B. Verma and H. Lal, *J. Mater. Sci. Lett.* 5 (1986) 783-784.
23. P. Battle, A. cheetham, W. Harrison, N. Pollard and J. Faber, *J. Solid State Chem.* 58 (1985) 221-225.
24. T.S. Popov, B.I. Popov, V.N. Bibin, G.M. Bliznakov, G.K. Boreskov, *React. Kinet. Catal. Lett.*3 (1975) 169-175.
25. J. Walczak, M. Kurzawa and E. Filipek, *Thermochim. Acta.*150 (1989) 133-140.
26. J. Peng, M. Wu, H. Wang. Y. M. Hao, Z.Hu, Z. X. Yu, D. F. Chen, R. Kiyanagi, J. S. Fieramosca, S. Short, J. Jorgensen, *J. Alloys. Compd.* 453 (2008) 49-54.
27. W. Doyle, G. McCurie, G. Clark, *J. Inorg. Nucl. Chem.* 28 (1966) 1185-1190.
28. N. Kadiri, A. Ben Ali, M. Abboudi, E. Moran, *Phys. Chem. News* 44 (2008) 11-14.
29. M. Abboudi, M. Messali, N. Kadiri, A. Ben Ali, E. Moran, *Synth. React. Inorg. Met.-Org. Chem.* 41 (2011) 683-688.
30. M. Messali, F. Al Wadaani, H. Oudghiri-Hassani, S. Rakass, S. Al Amri, M. Benaissa, M. Abboudi, *Mater. Lett.*128 (2014) 187-190.
31. K. Nakamoto, Infrared spectra of inorganic and coordination compounds, Wiley, New York, 1970, p. 245.
32. K. Y. S. Ng , X. Zhou , E. Gulari, *J. Phys. Chem.* 89 (1985**)** 2477–2481.
33. J. T. Andre Angermann, *Ceram. Int.* 37 (2011) 995–1002.
34. S. Onodera, Y Ikegami, *Inorg. Chem.* 19 (1980) 615-618.
35. D. Klissrski, M. Mancheva, R. Iordanova, B. Kunev, *Chem. for Sust. Devel.* 20(2005) 229-232.

(2018) ; http://www.jmaterenvironsci.com